Proceedings of the 1998 IEEE
International Conference on Robotics & Automation
Leuven, Belgium • May 1998

High Speed Tracking Control of Stewart Platform Manipulator via Enhanced Sliding Mode Control

Nag-In Kim* and Chong-Won Lee**

* Daewoo Heavy Industries Ltd., 6, Manseok-dong, Tong-gu, Incheon, South Korea, 401-010
Tel:+82-42-869-3056;Fax:+82-42-869-8220; E-mail:s_nikim@cais.kaist.ac.kr
** Center for Noise and Vibration Control, Department of Mechanical Engineering
KAIST, Science Town, Taejon, South Korea, 305-701
Tel:+82-42-869-3016;Fax:+82-42-869-8220; E-mail:cwlee@hanbit.kaist.ac.kr

Abstract: High speed tracking control of a 6-6 Stewart platform manipulator is performed by employing an enhanced sliding mode control with reduced manipulator dynamics when the manipulator is assumed to be operated on a low frequency planar motion unit. The high-performance tracking control strategy normally requires the complex full dynamics of 6-6 Stewart platform manipulator. The dynamics becomes even more complicated in the presence of the base motion of the manipulator, requiring additional sensors for measurement of the base motion. It is shown that enhanced sliding mode control implemented with perturbation compensation and reaching phase alleviation functions can effectively remove the use of the complex full dynamics and the additional sensors in the control system for high performance tracking control of the Stewart platform manipulator under the effects of virtual base motion.

1. INRODUCTION

In recent years, there has been considerable interest in the area of parallel manipulator, which provides better accuracy, rigidity, load-to-weight ratio, and load distribution than serial manipulator. Such advantages of fully parallel manipulators[1] originate from the fact that the actuators act in parallel sharing the common payload. Thus, parallel manipulators have been often used for high speed, high precision and large payload environments. Practical usage of the Stewart platform manipulator(SPM), the most famous 6 degree-of-freedom parallel manipulator, has generally been in the area of low speed and large payload conditions such as motion base of the classical automobile[2] or flight simulator, and motion bed of a machine tool[3]. In such applications, simple independent joint-axis PID or/and adaptive control[4], without knowledge of the complex dynamics in the design of the controller, have been widely adopted because the driving force required for generation of the desired motion is mostly consumed to compensate for the gravity force associated with the payload and external disturbance forces. However, high-performance tracking control of the high speed motion base used in enhanced automobile simulators and multi-axes vibration isolators generally necessitates the knowledge of the complex dynamics and the model-based controller.

The real time calculation of forward kinematics[5] and dynamics of SPM may be a difficult task owing to the time consuming nature. Lee and Kim[6] proposed the dual-processors based computing architecture to resolve the problem and introduced the joint-axis sliding mode control(SMC). On the other hand, SPM may be operated on a moving vehicle[7] or a low speed motion unit while the dynamics of the SPM is derived with the assumption that the lower base of the SPM is fixed to the inertia coordinates. Although such manipulators may normally experience low frequency base motion, large unpredictable dynamic force may exert to the system and the induced large tracking errors can not be avoided by the conventional SMC.

In this work, large tracking errors are effectively reduced by incorporating the reaching phase alleviation[8] and perturbation compensation[9] functions into the conventional SMC based on fixed base motion dynamics of the SPM. The reaching phase alleviator, which changes the conventional sliding surface to an augmented one during initial transient period, keeps the sliding function inside the boundary layer, or on the sliding surface, from start time, and thus it may alleviate the reaching phase of sliding mode control. The perturbation estimator effectively estimates the low frequency perturbation when the sliding function stays inside the boundary layer and then continuously compensates them in the control law. Using this enhanced SMC, the tracking control based on the fixed base motion dynamics is performed with the SPM and its high tracking control performance is proven experimentally.

2. CONTROL SYSTEM DESIGN

SPM configurations

The linear actuator system consisting of an AC servo motor and a linear ball screw system is employed in the laboratory SPM. The AC servo motor(Max. power: 200W) equipped with a 3000 pulse encoder generates torque and rotational motion, and the linear ball screw system(lead: 25mm) converts them into linear force(Max. rated force:240N; Peak force:720N) and linear motion. The motion range and dimensions of the SPM are given in Table 1 and Fig.1, respectively.

Table 1 Maximum one degree-of-freedom displacements of SPM

	Displacement, m		Displacement, °
x	+0.13 ◁▷ − 0.12	α	+9.8 ◁▷ −9.8
y	+0.11 ◁▷ − 0.11	β	+11.2 ◁▷ −9.2
z	+0.82 ◁▷ +0.72	γ	+21.5 ◁▷ −21.5

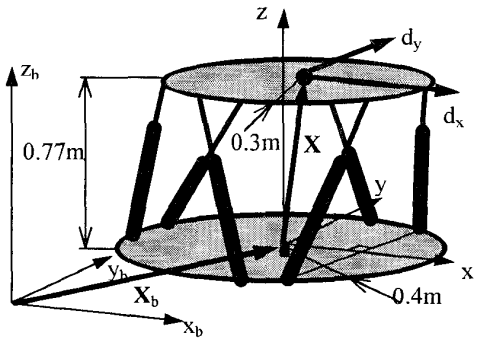

Figure 1 Stewart platform manipulator and the coordinates

Kinematics and Dynamics of SPM system

For the linear actuator system modeling, we consider only inertia and proportional friction terms, leaving other complex nonlinear behavior parts to the unknown perturbation. Lee and Kim[6] proposed the control system for the SPM that includes the iterative Newton-Raphson(NR) method[5] for the forward kinematics and the algebraically operated SPM dynamics including actuator dynamics, which basic form was proposed by Zhang and Song[10] expressed as

$$u_j(t) = \sum_{k=1}^{6}\left\{m_{jk}(\mathbf{X}(t))\ddot{l}_k(t)\right\} + V_j\left(\mathbf{X}(t),\dot{\mathbf{X}}(t),\dot{l}_j(t)\right) + G_j(\mathbf{X}(t)), \quad j = 1,2,\cdots,6 \qquad (1)$$

which can be used for design of the joint-axis control system. Here u_j denotes the actuated force; $\mathbf{X} = [x \;\; y \;\; z \;\; \alpha \;\; \beta \;\; \gamma]^T$ and $\dot{\mathbf{X}}$ are the coordinate and velocity vectors of the upper centroid, respectively; α, β and γ are the rotational angles about x, y and z axis, respectively; $\dot{l}_j$ and $\ddot{l}_j$ are the velocity and acceleration of actuator length, respectively; $[m_{jk}] \in R^{6x6}$ represents the inertia mass matrix of the SPM system, which is symmetric and nonsingular; $[V_j] \in R^{6x1}$ corresponds to frictional force of the actuator system, the centrifugal and Coriolis force vectors of the SPM system; $[G_j] \in R^{6x1}$ is the gravity force.

Control hardware and software

A model based control strategy generally needs calculation of system dynamics at every fixed sampling time interval. However, the SPM dynamics including numerical forward kinematics is generally difficult to calculate within a given sampling time interval. Thus, to reduce this difficulty, control architecture for the SPM control has been proposed as shown in Fig. 2[6]. The forward kinematic and dynamic equations are calculated on a PC(Pentium 133MHz) asynchronously to a DSP that is a general digital servo controller associated with TMS320C40, ADCs, DACs and counters. The PC provides the dynamic properties of the SPM, with a little uncertainty induced by the asynchronous calculation, to the digital servo controller without processing interference. Thus it can achieve a high speed feedback loop and design the model based control system for the SPM

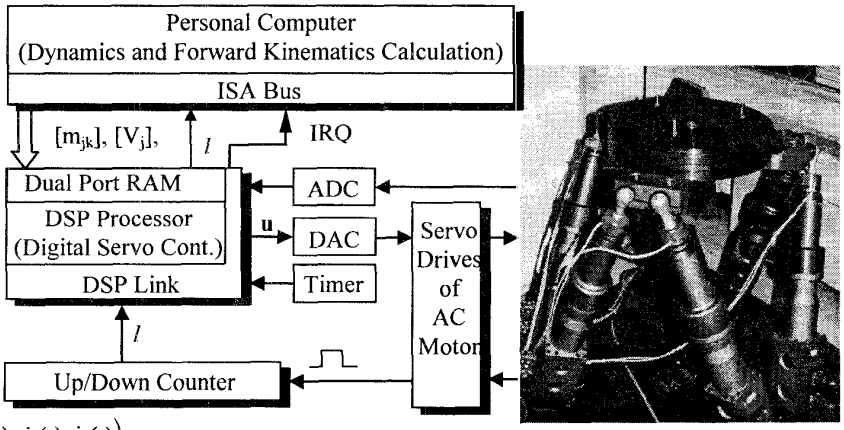

Figure 2 Control block diagram of SPM

Design of the conventional SMC

The dynamic system (1) can be re-written, in the presence of perturbation, as

$$u_j(t) = \sum_{k=1}^{6}\left\{m_{jk}(\mathbf{X}(t))\ddot{l}_k(t)\right\} + V_j\left(\mathbf{X}(t),\dot{\mathbf{X}}(t),\dot{l}_j(t)\right) + G_j(\mathbf{X}(t)) + \sum_{k=1}^{6}\left\{\Delta m_{jk}\ddot{l}_k\right\} + \Delta V_j\left(\mathbf{X}(t),\dot{\mathbf{X}}(t),\dot{l}_j\right) + \Delta G_j(\mathbf{X}(t)) + d_j(t)$$
$$j = 1,2,\cdots,6 \qquad (3)$$

Here Δm_{jk}, ΔV_j and ΔG_j are the uncertainties of m_{jk}, V_j and G_j, respectively, and d_j denotes the external disturbance. The sliding function s is defined by[8,11]

$$s_j = \dot{e}_j + \lambda_j e_j - g_j(t) \quad j = 1,2,\cdots,6 \qquad (4)$$

where $e_j = l_j - l_{d,j}$, the positive constant λ_j is the desired control bandwidth, l_j and $l_{d,j}$ are the measured and desired actuator lengths, and $g_j(t)$ is the reaching phase alleviation term defined as[8]

$$g_j(t) = \left\{\dot{e}_j(0) + \lambda_j e_j(0)\right\} exp\left(-\varphi_j t\right) \qquad (5)$$

where the positive definite φ_j is a time constant. Let the time derivative of the Lyapunov function candidate be given by $\frac{1}{2}\frac{d\left(s_j^2\right)}{dt} < 0$ to satisfy the boundary layer attraction condition, which gives the conventional SMC law defined as

$$u_j = \sum_{k=1}^{6}\left\{m_{jk}\left(\ddot{l}_{d,k} - \lambda_k \dot{e}_k + \dot{g}_k\right)\right\} - k_j \mathrm{sat}\left(s_j, s_{o,j}\right) + V_j + G_j, \quad j = 1,2,\cdots,6 \qquad (6)$$

where

$$k_j > max\left|\sum_{k=1}^{6}\left(\Delta m_{jk}\ddot{l}_k\right) + \Delta V_j + \Delta G_j + d_j\right| \qquad (7)$$

Here the positive constant s_o is the thickness of boundary layer[11].

Sliding mode control with perturbation compensation

Now, we introduce the SMC with perturbation compensation which was first proposed by Kim *et al.*[9]. The actual perturbation, $P_{E,j}$, may be divided into known, or estimated, and residual perturbations, Φ_j and $\Delta P_{E,j}$, *i.e.*

$$P_{E,j} = \Phi_j + \Delta P_{E,j} \qquad (8)$$

where

$$P_{E,j} = \sum_{k=1}^{6}\left\langle\left[b_{jk}\right]\left\{\sum_{i=1}^{6}\left(\Delta m_{ki}\ddot{l}_i\right) + \Delta V_k + \Delta G_k + d_k\right\}\right\rangle \quad \text{with} \quad \left[b_{jk}\right] = \left[m_{jk}\right]^{-1}$$

Then equation (6) becomes

$$u_j = \sum_{k=1}^{6} m_{jk}\left\{\ddot{l}_{d,k} - \lambda_k \dot{e}_k + \dot{g}_k - \Phi_j\right\} - k_{r,j}\mathrm{sat}\left(s_j, s_{o,j}\right) + V_j + G_j \qquad (9)$$

with the boundary layer attraction condition defined as

$$k_{r,j} > max\left|\Delta P_{E,j}\right| \qquad (10)$$

The structure of the controlled system is schematically shown in Fig. 3.

Dynamic system (3) may be divided into two parts: modeled and perturbation dynamic parts given by

$$u_{n,j} = \sum_{k=1}^{6}\left(m_{jk}\ddot{l}_{n,k}\right) + V_j + G_j \qquad (11.a)$$

$$u_{p,j} = \sum_{k=1}^{6}\left\{m_{jk}\left(\ddot{l}_{p,k} + P_{E,k}\right)\right\} \qquad (11.b)$$

Here $l_j = l_{n,j} + l_{p,j}$, $l_{p,j}$ and $l_{n,j}$ are the coordinate vectors associated with the modeled and perturbation dynamics, respectively, $u_{n,j}$ and $u_{p,j}$ are the corresponding control forces. The perturbation dynamics does not allow the state of dynamic system to stay on the sliding surface, *i.e.* $s \neq 0$, whereas the modeled dynamics can be completely compensated by the Filippov's equivalent dynamics[11] inside boundary layers, *i.e.* $\dot{s} = 0$. Thus the s of the original system can be expressed by the state of perturbed dynamics given, inside boundary layers, as

$$s_j = \dot{l}_{p,j} + \lambda_j l_{p,j} - g_j \quad j = 1,2,\cdots,6. \qquad (12)$$

If a well-designed controller for the perturbation dynamic system can generate the control force $u_{p,j}$ that

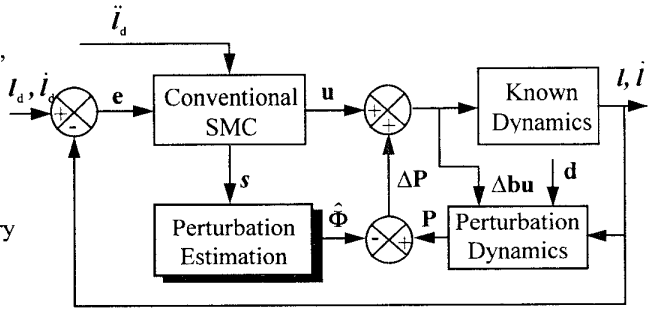

Figure 3. Structure of the proposed SMC system

drives the control states to its origin allowing only high-frequency errors, then most of low frequency perturbation acted upon the system is likely to be compensated by the control action. Thus the control force essentially reflects the relatively low frequency components of actual perturbations. It will prove convenient to introduce the relation

$$\ddot{l}_{p,j}(t) = -P_{E,j}(t) - \Phi_j(t), \quad j = 1,2,\cdots,6 \qquad (13)$$

where $\Phi_j = -\sum_{k=1}^{6}\left\{\left[b_{jk}\right]u_{p,k}\right\}$. Since the terms Φ_j also contain undesirable high frequency components owing to control action, an observer is proposed as

$$\dot{\hat{\Phi}}_j(t) + \omega_{n,j}\hat{\Phi}_j(t) = \omega_{n,j}\Phi_j(t), \quad j = 1,2,\cdots,6 \qquad (14)$$

Here $\hat{\Phi}_j$ is the filtered output of Φ_j and $\omega_{n,j}(\mathrm{rad/sec})$ is the filter frequency which indicates the frequency bandwidth for perturbation estimation.

The controlled dynamics of the form, for Φ_j,

$$\ddot{l}_{p,j}(t) + a_{j1}\dot{l}_{p,j}(t) + a_{j2}l_{p,j}(t) + g_{m,j}(t) = 0, \quad j = 1,2,\cdots,6 \qquad (15)$$

The coefficients, a_{j1} and a_{j2}, make the perturbation dynamic response asymptotically decay to its origin on the sliding surface, and $g_{m,j}$ is a time variable function. Substituting equation (13) into equation (15), we obtain

$$\Phi_j(t) = -P_{E,j}(t) + a_{j1}\dot{l}_{p,j}(t) + a_{j2}l_{p,j}(t) + g_{m,j}(t), \quad j = 1,2,\cdots,6 \qquad (16)$$

Note here that we need the information of $P_{E,j}(t)$ to obtain $\Phi_j(t)$. TDC for slowly varying perturbations and system

dynamics[12] essentially assumes that, for a sufficiently small time delay Δt,

$$P_{E,j}(t) \cong P_{E,j}(t-\Delta t) = -\ddot{I}_{p,j}(t-\Delta t) - \Phi_j(t-\Delta t) \qquad j = 1,2,\cdots,6 \qquad (17)$$

The manipulator dynamics of interest possesses wide band frequency characteristics, so that the approximation (17) may not be valid. One of the simple, yet effective, remedies is to remove the high frequency components in $P_{E,j}$ by low-pass filtering. In other words, equation (17) may be replaced by

$$\hat{P}_{E,j}(t) \cong \hat{P}_{E,j}(t-\Delta t) = -\hat{\ddot{I}}_{p,j}(t-\Delta t) - \hat{\Phi}_j(t-\Delta t) \qquad (18)$$

where '^' indicates the low-pass filtered value. Substituting equations (18) and (16) into equation (14), we obtain[9]

$$\hat{\Phi}_j(t) \cong k_{p,j}\left[s_j(t) + h_j \int s_j(t)dt\right] \qquad (19)$$

for sufficiently small Δt and slow $\hat{\Phi}_j$. Here $k_{p,j} = \omega_{n,j}$, $a_{j1} = -(\lambda_j + h_j)$, $a_{j2} = -\lambda_j h_j$ and $g_{m,j} = -\dot{g}_j - h_j g_j$.

3. PROBLEM FORMULATION

In this study, SPM is to be used primarily as the motion generator of an aircraft or driving simulator. The driving simulator is known to have the smaller amplitude and higher frequency characteristics in the simulated motion than the aircraft simulator. Figure 1 shows the schematic layout and coordinates of a driving simulator running on the two degree-of-freedom planar motion unit. Thus, the two motion units share the desired motion, which is required by the automobile simulator, according to the system characteristics such that the SPM and the planar motion unit simulate the high and low frequency motions, respectively. Although the SPM simulates the high frequency motion, the inertia parts are exposed under the low frequency motion by the planar motion unit so that it leads the SPM dynamics to be a more complex one than equation (1).

Let us define the dynamics of the platform given as

$$\mathbf{u}_N(t) = \mathbf{u}(t) + \mathbf{M}_X(\mathbf{X})\ddot{\mathbf{X}}_b(t) + \Delta\mathbf{V}_X(\mathbf{X},\dot{\mathbf{X}},\dot{\mathbf{X}}_b) \qquad (20)$$

Here $\mathbf{u}_N(t)$ represents the actuated force vector considering base motion in deriving the SPM dynamic equation, $\dot{\mathbf{X}}_b = [\dot{x}_b \quad \dot{y}_b \quad 0 \quad 0 \quad 0 \quad 0]^T$ and $\ddot{\mathbf{X}}_b = [\ddot{x}_b \quad \ddot{y}_b \quad 0 \quad 0 \quad 0 \quad 0]^T$ represent the base velocity and acceleration vectors of the SPM, respectively, and $\Delta\mathbf{V}_X(\mathbf{X},\dot{\mathbf{X}},\dot{\mathbf{X}}_b) = \mathbf{V}_{NX}(\mathbf{X},\dot{\mathbf{X}},\dot{\mathbf{X}}_b) - \mathbf{V}(\mathbf{X},\dot{\mathbf{X}})$, $\mathbf{V}_{NX}(\mathbf{X},\dot{\mathbf{X}},\dot{\mathbf{X}}_b)$ is the Coriolis and centrifugal force vector in the presence of base motion, which may be a very small in value relative to other terms since the low dexterity of SPM. The term $\mathbf{M}_X(\mathbf{X})\ddot{\mathbf{X}}_b$, whose frequency characteristics closely resembles $\ddot{\mathbf{X}}_b$ that is sometimes difficult or/and expensive to measure, is the dominant dynamic force in dynamic equation (20) except **u**. Thus we treat $\mathbf{M}_X(\mathbf{X})\ddot{\mathbf{X}}_b$ as an unmodelled dynamics in this study to simplify the SPM modeling, without using feedback sensors to measure $\ddot{\mathbf{X}}_b$.

4. EXPERIMENT

To check the controllability of the proposed controller, control experiments were performed under the given command trajectory:

$$\begin{cases} x(t) = 0.03\{1-exp(-\pi t)\}cos(1.88\pi t), & m \\ y(t) = 0.04\{1-exp(-\pi t)\}sin(1.88\pi t), & m \\ z(t) = \dfrac{0.02}{1+0.9t}sin\left\{2\pi t\left(\dfrac{0.1+5.9t}{10.5}\right)+\dfrac{\pi}{24}\right\}, & m \\ \alpha(t) = 0, \quad deg \\ \beta(t) = 4\{1-exp(-\pi t)\}sin(0.86\pi t), & deg \\ \gamma(t) = 5\{1-exp(-\pi t)\}sin(0.74\pi t), & deg \end{cases} \quad ;0 \le t \le 10$$

$$x(t) = y(t) = z(t) = \alpha(t) = \beta(t) = \gamma(t) = \gamma(t) = 0 \quad ;\text{otherwise} \qquad (21)$$

The control parameter values throughout the tests are: $\lambda_j = 14\pi\,\text{rad}/sec$, $s_{o,j} = 0.06\,m/sec$, $k_j = k_{r,j} = 160\,N$, $\omega_{n,j} = 3\pi\,\text{rad}/sec$, and $h_j = \lambda_j = \varphi_j$, thus $g_{m,j} = 0$, for j=1,2, ..., 6. The payload of SPM is 64 kg. To simulate the effects of the base motion, the centroid of upper platform of the manipulator is assumed to be subjected to the disturbance forces, d_x and d_y, along the x and y directions, respectively, given by

$$\begin{Bmatrix} d_x \\ d_y \end{Bmatrix} = \begin{bmatrix} 180sin(0.86\pi t) + 120sin(1.26\pi t) \\ 150sin(1.06\pi t) + 80sin(1.74\pi t) \end{bmatrix}, \quad N \qquad (22.a)$$

In fact, such disturbance forces can be experienced by the manipulator, for example, when the base motion of SPM is exposed to the disturbance motions, x_b and y_b, given by

$$\begin{Bmatrix} x_b \\ y_b \end{Bmatrix} = \begin{bmatrix} -0.385sin(0.86\pi t) - 0.12sin(1.26\pi t) \\ -211sin(1.06\pi t) - 0.048sin(1.74\pi t) \end{bmatrix}, \quad m \qquad (22.b)$$

Because most of time consuming routines are executed asynchronously by a PC, we can carry out the control task within the sampling time interval of 1 m*sec*. The asynchronous task executed by the PC required about 2-3 m*sec* to finish its all routines. Figures 4-7 show the tracking errors in the operating coordinates, the typical sliding functions associated with the tracking errors in the actuator direction coordinates, the typical actuator control

forces and the estimated virtual perturbations. Although both the conventional and enhanced SMCs did not induce chattering in the control input, the former failed in effectively rejecting the low frequency perturbations. Note that the enhanced SMC resulted in relatively smaller tracking errors and s values than the conventional SMC owing to its capability of rejecting the low frequency perturbation. Figure 6 shows that the time-varying sliding surface enables the estimated perturbation to exponentially track the actual low frequency perturbation in the initial start time period, and the estimated perturbations successfully track the large external disturbances that are the major source of tracking errors during the steady state. It implies that the control system was eventually subjected only to the small residual perturbation. The s value associated with the enhanced SMC remained inside the pre-defined boundary layer throughout the control test whereas the s value for the conventional SMC often violated the boundary layer attraction condition owing to the virtually low frequency and large external disturbances. It indicates that the low frequency external disturbances do not affect the tracking performance of the enhanced SMC, and the upper bound of the perturbation k_j in the conventional SMC should be increased until the boundary layer attraction condition is satisfied, that, in turn, may cause poor tracking performance and undesirable control oscillations.

5. SUMMARY AND CONCLUSIONS

The enhanced SMC and proposed control system was shown to be an effective approach for model based tracking control of the SPM, which is exposed to a low frequency base motion. Employing the enhanced SMC, we treated the dynamic part induced by low frequency base motion as an unmodelled dynamics of the SPM, which was then effectively compensated in the controller by the augmented sliding surface and perturbation estimation. It lead us to use the simple SPM dynamics in the control law, so that the control system became simple when the SPM runs on a low frequency planar motion unit. Experimental results confirmed that the control system with implemented the enhanced SMC allowed us to design a simple high-performance tracking control system for the SPM system under the high payload and large disturbance conditions.

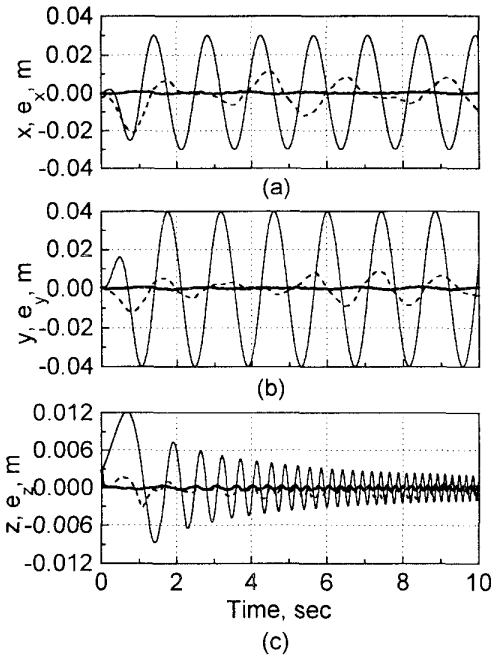

Figure 4 Typical tracking Errors: —— Command, – – Conventional SMC($\hat{\Phi} = 0$), ▬▬ Enhanced SMC

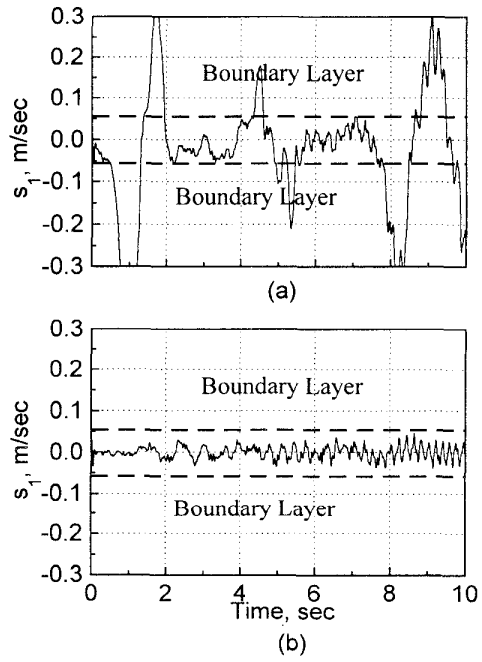

Figure 5 Typical sliding functions:
(a) Conventional SMC $\left(\hat{\Phi} = 0\right)$, (b) Enhanced SMC

REFERENCES

[1] D. Stewart, A Platform with six degree of freedom, Proceedings of the Institution of Mechanical Engineering, Vol. 180, Part 1, No. 5, 1965, pp. 371-386.

[2] S. Freeman *et al.,* The Iowa driving simulator: An implementation and application overview, 1995, SAE 950174, pp. 1-10.

[3] G. Lebret, K. Liu and F. L. Lewis, Dynamic analysis and control of a Stewart platform manipulator, Journal of Robotic System, 1993, Vol. 10, No. 5, pp. 629-656.

[4] C. C. Nguyen, S. S. Antrazi, X.-L. Xhou and C. E. campbell, Jr., Adaptive control of a Stewart platform-based manipulator, Journal of Robotic System, 1993, Vol. 10, No. 5, pp. 657-668 .

[5] R. V. Parrish, J. E. Dieudenne and D. J. Martin, Jr., Motion software for a synergistic six-degree-of-freedom motion base, NASA TN D-7350, 1973.

[6] C. W. Lee and N. I. Kim, Model based sliding mode control of Stewart platform manipulator, Korea Automatic Control Conference 97.

[7] J. Bormann and H. Ulbrich, Isolation of vibrations to avoid dynamic interactions between a telescope and its foundation by active control, Third International Conference on Motion and Vibration Control, 1996, pp. 88-93.

[8] K. B. Park and J. J. Lee, Variable structure controller for robot manipulators using time-varying sliding surface, IEEE Conference on Robotics and Automation, 1993, pp. 89-93.

[9] N. I. Kim, C. W. Lee and P. H. Chang, Tracking control of the parallel manipulator by sliding mode control with perturbation estimation, Submitted to Control Engineering Practice.

[10]C.-D. Zhang and S.-N. Song, An efficient method for inverse dynamics of manipulator based on virtual work principle, Journal of Robotic System, 1993, Vol. 10, No. 5, pp. 605-628.

[11]J.-J. E. Slotine, Sliding controller design for non-linear systems, International Journal of Control, Vol. 40, No. 2, 1984, pp. 421-434.

[12]K. Youcef-Toumi and O. Ito, A time delay controller for systems with unknown dynamics, ASME Journal of Dynamic Systems, Measurement, and Control, Vol. 112, 1990, pp. 133-142.

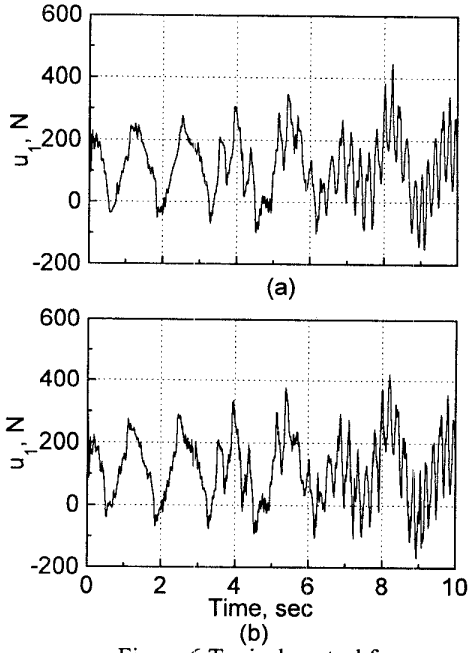

Figure 6 Typical control forces:
(a) Conventional SMC $\left(\hat{\Phi}=0\right)$, (b) Enhanced SMC

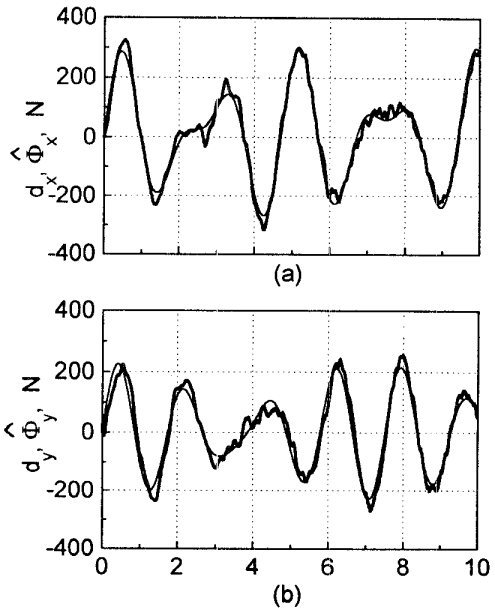

Figure 7 Applied and estimated forces: (a)x direction, (b)y direction forces
—— Applied disturbance $\left(d_x, d_y\right)$, ━━ Estimated disturbance $\left(\hat{\Phi}\right)$